

# Penetration Theory for Inclined and Moving Shaped Charges

M. Held and R. Fischer

Messerschmitt-Bölkow-Blohm GmbH, D-8898 Schrobenehausen (West Germany)

## Theorie der Eindringtiefe von geneigten und bewegten Hohlladungen

Es wird ein analytisches Modell für die Berechnung der sogenannten dynamischen Eindringtiefe von zur Flugrichtung geneigten Hohlladungen für kleine und große Abstände zum Ziel und auch gegenüber geneigten Zielplatten gegeben.

Der Vorteil eines derartigen analytischen Modells ist, daß die Eindringtiefen abgeschätzt und die Trends bei Änderung der Hohlladungs- und Zielparame-ter einfach und schnell bestimmt werden können.

## Théorie de la pénétration des charges creuses inclinées et animées d'un mouvement de translation

On décrit un modèle analytique permettant de calculer la profondeur de pénétration dite «dynamique» de charges creuses inclinées par rapport à leur direction de vol, pour une quelconque distance d'action et pour différents, angles d'incidence par rapport au blindage.

L'avantage d'un tel modèle analytique réside dans le fait qu'il fournit une évaluation de la profondeur de pénétration et qu'il permet de déterminer rapidement et de manière simple les résultats à escompter à la suite d'une variation des paramètres caractéristiques de la charge creuse ou de la cible.

## Summary

An analytical model will be given for the calculation of the dynamic penetration of inclined shaped charges at an arbitrary stand-off distance and for all possible angles between the shaped charge axis and the axis of the carrier, and for various obliquities of the target plate.

The advantage of an analytical model is, estimates of penetration and trends can be established quickly and easily through a variation of shaped charge and target parameters.

## 1. Introduction

Defeating the heavy armor, or even the special armor, on main battle tanks would require a perforation capacity and, hence, the weight of a mono shaped charge warhead, that is no longer practicable with portable or even vehicle-launched guided missiles. Apart from special shaped charge systems and multiple shaped charges, the low altitude-flight or dive-attack mode can be used in fighting such targets. The latter attack mode requires a seeker which may interfere with good jet formation and, therefore, also may reduce the performance of an axial shaped charge warhead. To avoid this disturbing effect of a seeker and still enable a missile to fly over a target almost horizontally, an investigation has been made into the feasibility of a design, in which a shaped charge is built into the missile obliquely to the missile axis (Fig. 1). However, such an arrangement of the shaped charge results in a cutting action of the shaped charge jet in the target. The cutting length depends on the stand-off distance from the target and on the flight velocity of the missile. In certain cases, this may lead to a considerable drop in penetration performance of the weapon.

The dynamic penetration of a shaped charge that is arranged at an angle of  $90^\circ$  to the missile axis, has previously been derived in detail in Ref. 1. In this analysis the performance against a target plate parallel to the missile axis and perpendicularly to the direction of jet propagation is presented. In this Reference 1 the distance from the charge to the target was assumed to be so long, that the shaped charge jet would always be articulated.

Below, the formulas presented in Reference 1 are generalized for a shaped charge inclined at an arbitrary angle to the missile axis and for target plates also placed at an arbitrary oblique angle to the missile axis. Now, the case of a continuous

jet which applies to closer stand-off distances, can also be described by the modified equations.

The advantage of an analytical model is, that trends through a variation of parameters can be established more quickly and easily, than by means of the statistical models according to Smith and Goleworthy<sup>(2,3)</sup>. There, each and every firing trial must be calculated separately. To obtain a representative result, one would have to carry out several tests with a range of parameters in order to obtain a statistical average. This involves a considerably greater effort of calculation and clear insight into trends and tendencies is obtained.

## 2. Effect of the Angle

The definitions of the angles, as used below, are shown in Fig. 2. A missile is assumed to fly with velocity  $v_m$  at an angle  $\alpha$  with respect to the horizontal. For simplicity, the velocity vector in Fig. 2 is assumed to point in the same direction as the missile axis. The shaped charge itself is inclined at an angle  $\beta$  to the flight trajectory, which in this case is coincident with the missile axis. The target plate slants at angle  $\varepsilon$  to the horizontal.

In the dynamic case, the jet tip velocity  $v_{j,\beta}^1$  in the direction of the shaped charge axis is the vectorial sum of the jet tip velocity  $v_j^1$  of the shaped charge for the static case and the velocity  $v_m$  of the missile (Fig. 2):

$$v_{j,\beta}^1 = v_j^1 + v_m \cdot \cos \beta \quad (1)$$

The velocities  $v_{j,\perp}^n$  of the individual jet elements perpendicularly to the shaped charge axis all correspond to the sine of the missile velocity  $v_m$ :

$$v_{j,\perp}^n = v_{m,\perp} = v_m \cdot \sin \beta \quad (2)$$

The length  $x_c$  of the cut perpendicular to the axis of the shaped charge made by the  $n$ -th jet element in the target, results from the deviation  $x_n$  of this  $n$ -th particle of the jet with respect to the deviation  $x_1$  of the tip of the jet due to the flight velocity of the missile:

$$x_c = x_n - x_1 \quad (3)$$

**Figure 1.** Warheads with shaped charges arranged obliquely with respect to the missile or projectile axis. This type of arrangement is intended for attacking targets in the low-altitude or direct-attack mode. The jet disturbances due to the penetration of the seeker are eliminated, the target is attacked at its most vulnerable side and the special armor will show less effect.

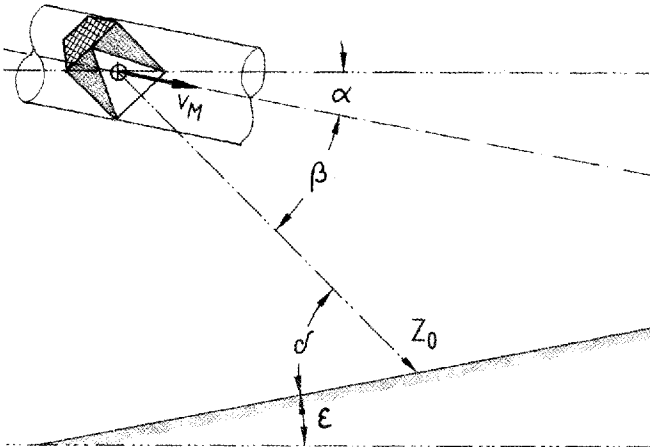


**Figure 2.** Definition of the parameters and angles. Positive angles in clockwise direction.

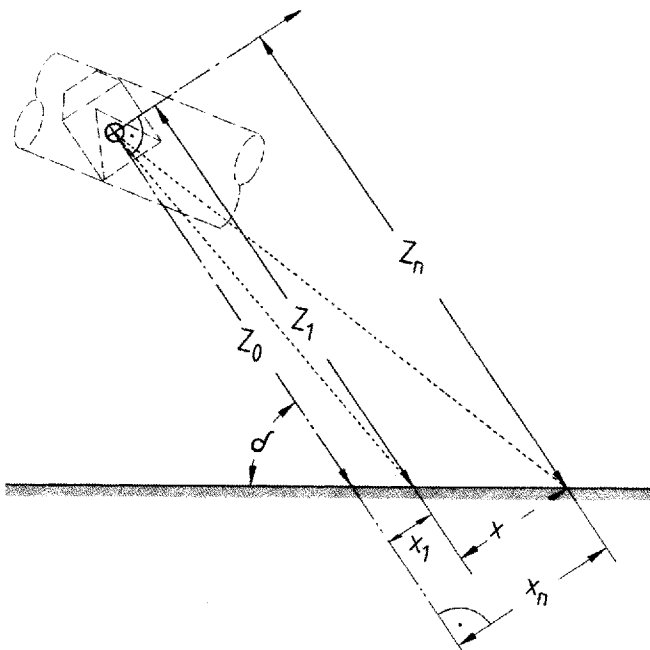


**Figure 3.** Definition of the distance from the virtual origin of the shaped charge to the target surface,  $Z_i$  and of the dynamic jet deviations,  $x_i$ .

Here, the deviation  $x_n$  is calculated by multiplying the missile velocity component  $v_{m,\perp}$  perpendicular to the shaped charge axis and the flight time of the associated particle (Fig. 3). The expression for  $x_c$  can then be written as:

$$x_c = v_{m,\perp} \cdot (t_n - t_1) \quad (4)$$

The flight time follows from the distance the particle has travelled from where it was generated – for simplicity this is its virtual origin – and from the flight velocity  $v_{j,\beta}^n$  of that particle, i.e.

$$x_c = v_{m,\perp} \cdot \left( \frac{Z_n}{v_{j,\beta}^n} - \frac{Z_1}{v_{j,\beta}^l} \right) \quad (5)$$

This formula is still very similar to the one derived in Reference 1, the only difference being that new distances  $Z_n$  and  $Z_1$  must be considered, because now the target plate is no longer perpendicular to the axis of the shaped charge.

The  $Z_i$  are the flight distances of the jet particles parallel to  $Z_0$ , which correspond to the velocities  $v_{j,\beta}^n$  as solid lines in this direction. It should be noted that these are not the hypotenuses drawn in Fig. 3 between the virtual origin and the impact points as dotted lines. Along these diagonal lines, the jet elements have the vectorial sum of  $v_{j,\beta}^n$  and  $v_{m,\perp}$  as their velocity, instead of  $v_{j,\beta}^n$  alone.

It is clear from Fig. 3 that  $Z_i$  can readily be calculated as a function of  $Z_0$ ,  $x_i$  and the angle  $\delta$ :

$$Z_i = Z_0 + x_i \cdot \text{ctg } \delta \quad (6)$$

where, according to Fig. 2,  $\delta$  is given by

$$\delta = \alpha + \beta - \epsilon \quad (7)$$

The angles are positive in the clockwise direction.

For  $x_i$  one can also write

$$x_i = Z_i \cdot \frac{v_{m,\perp}}{v_{j,\beta}^l} \quad (8)$$

By inserting Eq. (8) into Eq. (6) and solving for  $Z_i$  one obtains

$$Z_i = \frac{Z_0}{1 - \text{ctg } \delta \cdot \frac{v_{m,\perp}}{v_{j,\beta}^l}} \quad (9)$$

The distances  $Z_i$  can now be inserted in Eq. (5). This leads to the following expression for the length of the cut  $x_c$ :

$$x_c = v_{m,\perp} \cdot Z_0 \cdot \left[ \frac{1}{v_{j,\beta}^n - v_{m,\perp} \cdot \text{ctg } \delta} - \frac{1}{v_{j,\beta}^l - v_{m,\perp} \cdot \text{ctg } \delta} \right] \quad (10)$$

This equation can be solved for the residual velocity  $v_{j,\beta}^n$ , that produces exactly this length of cut,  $x_c$ . In this equation,

$v_{j,\beta}^n$  is a function of the jet tip velocity  $v_{j,\beta}^1$ , the missile velocity perpendicularly to the axis of the jet,  $v_{m,\perp}$  equal to  $v_m \cdot \sin \beta$ , the distance  $Z_0$ , and the angles  $\alpha$ ,  $\beta$  and  $\epsilon$ , or their sum,  $\delta$ :

$$v_{j,\beta}^n = v_{m,\perp} \cdot \operatorname{ctg} \delta + \left[ \frac{1}{\frac{x_c}{v_{m,\perp} Z_0} + \frac{1}{v_{j,\beta}^1 - v_{m,\perp} \operatorname{ctg} \delta}} \right] \quad (11)$$

or

$$v_{j,\beta}^n = v_{m,\perp} \cdot \operatorname{ctg} \delta + \left[ \frac{v_{j,\beta}^1}{\frac{x_c}{Z_0} \cdot \frac{v_{j,\beta}^1}{v_{m,\perp}} + \frac{1}{1 - \frac{v_{m,\perp}}{v_{j,\beta}^1} \cdot \operatorname{ctg} \delta}} \right] \quad (12)$$

This  $v_{j,\beta}^n$  corresponds to the minimum velocity,  $v_{j,\min}$ , which in Ref. 1 occurs in Eqs. (1), (4), and (7). Thus,  $v_{j,\beta}^n$  is an extension of the formulas in Ref. 1 for shaped charges arranged at arbitrary angles to the missile axis and for target plates, that are placed at arbitrary angles to the flight direction of the inclined shaped charge carrier, e.g. a missile.

For the special case of a horizontal overfly ( $\alpha = 0^\circ$ ), a shaped charge directed vertically down ( $\beta = 90^\circ$ ), and for a horizontal target plate ( $\epsilon = 0^\circ$ ), the value of  $\delta$  is  $90^\circ$ , which means  $\cot \delta = 0$ ,  $v_{j,\beta}^n = v_j^n$  and  $v_{m,\perp} = v_m \cdot \sin \beta = v_m$ . Hence, the original formula [Eq. (4) from Ref. 1], is again obtained:

$$v_j^n = \left[ \frac{v_j^1}{\frac{x_c \cdot v_j^1}{Z_0 \cdot v_m} + 1} \right] \quad (13)$$

The correspondence between the variables is as follows:

| Present paper | Ref. 1       |
|---------------|--------------|
| $v_j^n$       | $v_{j,\min}$ |
| $v_j^1$       | $v_{j,0}$    |
| $v_m$         | $v_w$        |
| $Z_0$         | $D$          |

### 3. Impact Diameter

According to Ref. 1,  $x_c$  is equal to half the difference between the hole diameter in the target,  $D_T$ , minus the particle or jet diameter,  $D_p$ . This means, that only those jet portions contribute to the maximum depth of penetration, which are able to pass through the hole made by the previous jet portions. As soon as the jet begins touching the sides of the crater, the induced shock waves will disintegrate the jet, which will no longer contribute to the motion of the crater bottom.

When a shaped charge jet impinges perpendicularly, the crater formed is more or less symmetrical (Fig. 4a), as is known from many flash-X-ray shadowgraphs. When the jet hits the target obliquely, it will produce an unsymmetrical hole (Fig. 4b). If the jet has a negative inclination  $\delta$  toward the normal of the plate, then the hole on the surface of the plate will be torn up in the direction of motion much more than in the case of a symmetrical hole. However, the pattern of the hole size must in general not be analysed too close to the plate surface, because the edge effects of the spallation from the surface create a larger diameter hole. But the symmetrical

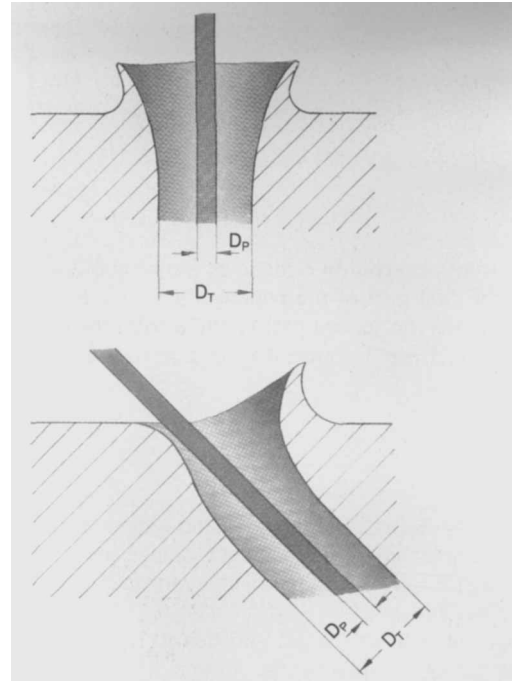


Figure 4. Cratering in a target that is arranged perpendicularly or obliquely to the axis of the jet.

small diameter hole appears already after a relatively short distance.

So the value of  $x_c$  is more or less rotationally symmetric about the impinging jet after a few centimeters of penetration, even when the plates are oblique with respect to the jet. It then corresponds to the value perpendicular to the trajectory of the jet, as given by the above equations. Thus,  $x_c$  must be taken in the direction of  $v_{m,\perp}$ . Therefore, the equations and formulas derived in Ref. 1 may be used for  $x_c$ . Hence

$$x_c = (D_T - D_p)/2 \quad (14)$$

where

$$D_T = v_{j,\beta}^1 \cdot D_p \cdot \sqrt{0.5 \cdot K \sqrt{Q_j} \cdot Q_T} \quad (15)$$

This leads to the following equation for the dynamic depth of penetration,  $P_{\text{dyn}}$ . This equation applies for the general case of a shaped charge, which is at an oblique angle to the flight direction, and for a target plate that is arranged arbitrarily:

One has to differentiate between the following 3 cases:

Case (1)

$$P_{\text{dyn}} = Z_1 \cdot \left[ \left( \frac{v_{j,\beta}^1}{v_{j,\beta}^n} \right)^{1/\gamma} - 1 \right] \quad (16a)$$

$$\text{for } Z_1 \leq v_{j,\beta}^n \cdot t_{p,s} \cdot D_C \cdot \left[ \frac{v_{j,\beta}^n}{v_{j,\beta}^1} \right]^{1/\gamma}$$

Case (2)

$$P_{\text{dyn}} = [(1 + \gamma) \cdot (v_{j,\beta}^1 \cdot t_{p,s} \cdot D_C)^{1/\gamma+1} Z_1^{\gamma/\gamma+1} - v_{j,\beta}^n \cdot t_{p,s} \cdot D_C] / \gamma - Z_1 \quad (16b)$$

$$\text{for } v_{j,\beta}^n \cdot t_{p,s} \cdot D_C \left[ \frac{v_{j,\beta}^n}{v_{j,\beta}^1} \right]^{1/\gamma} \leq Z_1 \leq t_{p,s} \cdot D_C \cdot v_{j,\beta}^1$$

## Case (3)

$$P_{\text{dyn}} = v_{j,\beta}^1 \cdot t_{p,s} \cdot D_C \cdot 1/\gamma \left[ 1 - \frac{v_{n,\beta}^n}{v_{j,\beta}^1} \right] \quad (16c)$$

$$\text{for } Z_1 > t_{p,s} \cdot D_C \cdot v_{j,\beta}^1$$

$$\text{with } \gamma = \sqrt{\rho_T/\rho_j}$$

In Case 1, the total penetration is made by a continuous jet. In Case 2, only the first part of the penetration is due to the continuous jet whereas the second part resulted from the particulated jet. Finally, Case 3 applies to the penetration of a fully particulated jet.

## 4. Diameter of the Jet

As soon as the jet has broken up, it does no longer stretch and, hence, its diameter  $D_p$  does no longer change. All that changes is the distance between the individual particles owing to their different velocities.

Since mass is conserved in the jet and density appears to remain constant during elongation, the volume also remains constant. Let us consider a certain jet element  $\Delta \ell_p$  after breakup of the jet with a certain velocity difference,  $\Delta v$ , and diameter  $D_p$ . Then, the following equation holds for the diameter  $D_p(\ell)$  of the jet element with the same velocity difference, if its length  $\Delta \ell$  has not yet grown much:

$$D_p(\ell) = D_p \cdot \sqrt{\Delta \ell_p / \Delta \ell} \quad (17)$$

As in the simple model with a virtual origin, i.e., where the jet is generated at time  $t = 0$ , the length  $\Delta \ell$  increases linearly with time  $t$  up to the break-up time  $t_p$ . Then the above equation can also be written as

$$D_p(t) = D_p \cdot \sqrt{t_p/t} \quad (17a)$$

When the stand-off-distance from the target is so small, that the jet has not yet broken up into particles ( $Z_1 < v_{j,\beta}^1 \cdot t_p$ ), the

diameter of the still-continuous jet can be calculated, if the diameter  $D_p$ , of the particulated, i.e. broken up jet is known. This is done by taking the square root of the ratio of length of the jet and length of the jet particles (at least in the region of the jet tip), or the ratio of break-up time,  $t_p$ , by impact time,  $t$ , and multiplying by the diameter of the particulated jet.

This will give a first, good approximation for determining the jet diameter as a function of distance for the continuous jet.

If one takes the change of jet diameter in consideration, the length of cut will be a function of the flight time  $t_n$ , of the  $n$ -th jet particle [Eq. (4)]. With

$$t_n = \frac{Z_n}{v_{j,\beta}^n} \quad (18)$$

$x_c$  becomes a function of  $v_{j,\beta}^n$ . This equation is not easily solvable for  $v_{j,\beta}^n$ . The computer-program solves this problem by means of iteration. In the first step, the diameter of the first particle is used for Eq. (15) and then  $v_{j,\beta}^{n1}$  is determined from Eqs. (14) and (11). Next, the diameter of the jet-particle with the velocity  $v_{j,\beta}^{n1}$  will be calculated and the Eqs. (15), (14) and (11) give  $v_{j,\beta}^{n2}$ . After a few iterative steps, the value for  $v_{j,\beta}^n$  converges.

## 5. Examples

With these formulas, trends and optimizations can be determined quite well, even if some of the parameters – like the proportionally factor  $K$  between volume and kinetic energy of the jet (or the V/KE-factor for short), must be determined from experiment. Below, the depths of penetration in a horizontal target plate (e.g. the top of a battle tank), the depth of penetration with 20° obliquity to the horizontal (e.g. a glacis plate) and the depth of penetration in an 80° oblique target plate (e.g. the turret armor) will be calculated as functions of the angle at which the shaped charge is inclined relatively to a missile flying horizontally. The following values of the parameters were chosen:

**Figure 5.** Example of a computer printout for the calculation of the “dynamic penetration performance” of shaped charges in a missile, that is moving parallel to a target plate at 300 mm stand-off distance and at a velocity of 300 mm/s; the shaped charge inclination being varied in steps of 5° to the missile axis. The printout also shows the values of  $Z_0$ ,  $Z_1$ ,  $v_{j,\beta}^1$ ,  $v_{j,\beta}^{n1}$ ,  $v_{j,\beta}^{n2}$ ,  $x_c$ ,  $P_{\text{dyn}}$  (in the direction of the jet), and  $P_N$  (normal to the plate).

| $\alpha$ | $\beta$ | $\varepsilon$ | $Z_0$  | $Z_1$  | $v_{j,\beta}^1$ | $v_{j,\beta}^{n1}$ | $v_{j,\beta}^{n2}$ | $x$   | $P_{\text{dyn}}$ | $P_N$  |
|----------|---------|---------------|--------|--------|-----------------|--------------------|--------------------|-------|------------------|--------|
| 0        | 5       | 0             | 3442.1 | 3556.4 | 9.299           | 0.026              | 5.908              | 6.04  | 722.03           | 62.93  |
| 0        | 10      | 0             | 1727.6 | 1784.3 | 9.295           | 0.052              | 5.852              | 6.20  | 732.57           | 127.21 |
| 0        | 15      | 0             | 1159.1 | 1196.6 | 9.290           | 0.078              | 5.320              | 7.89  | 770.47           | 199.41 |
| 0        | 20      | 0             | 877.1  | 904.6  | 9.282           | 0.103              | 4.948              | 9.29  | 747.71           | 255.73 |
| 0        | 25      | 0             | 709.9  | 731.3  | 9.272           | 0.127              | 4.667              | 10.48 | 714.73           | 302.06 |
| 0        | 30      | 0             | 600.0  | 617.3  | 9.260           | 0.150              | 4.443              | 11.51 | 682.52           | 341.26 |
| 0        | 35      | 0             | 523.0  | 537.3  | 9.246           | 0.172              | 4.261              | 12.42 | 653.75           | 374.98 |
| 0        | 40      | 0             | 466.7  | 478.6  | 9.230           | 0.193              | 4.108              | 13.21 | 628.87           | 404.23 |
| 0        | 45      | 0             | 424.3  | 434.3  | 9.212           | 0.212              | 3.979              | 13.89 | 607.71           | 429.72 |
| 0        | 50      | 0             | 391.6  | 400.0  | 9.193           | 0.230              | 3.868              | 14.49 | 589.91           | 451.90 |
| 0        | 55      | 0             | 366.2  | 373.2  | 9.172           | 0.246              | 3.772              | 15.00 | 575.11           | 471.10 |
| 0        | 60      | 0             | 346.4  | 352.2  | 9.150           | 0.260              | 3.690              | 15.42 | 562.98           | 487.56 |
| 0        | 65      | 0             | 331.0  | 335.7  | 9.127           | 0.272              | 3.620              | 15.77 | 553.27           | 501.43 |
| 0        | 70      | 0             | 319.3  | 322.9  | 9.103           | 0.282              | 3.559              | 16.04 | 545.72           | 512.81 |
| 0        | 75      | 0             | 310.6  | 313.3  | 9.078           | 0.290              | 3.509              | 16.23 | 540.18           | 521.77 |
| 0        | 80      | 0             | 304.6  | 306.4  | 9.052           | 0.295              | 3.467              | 16.35 | 536.47           | 528.32 |
| 0        | 85      | 0             | 301.1  | 302.0  | 9.026           | 0.299              | 3.435              | 16.40 | 534.50           | 532.46 |
| 0        | 90      | 0             | 300.0  | 300.0  | 9.000           | 0.300              | 3.411              | 16.39 | 534.17           | 534.17 |

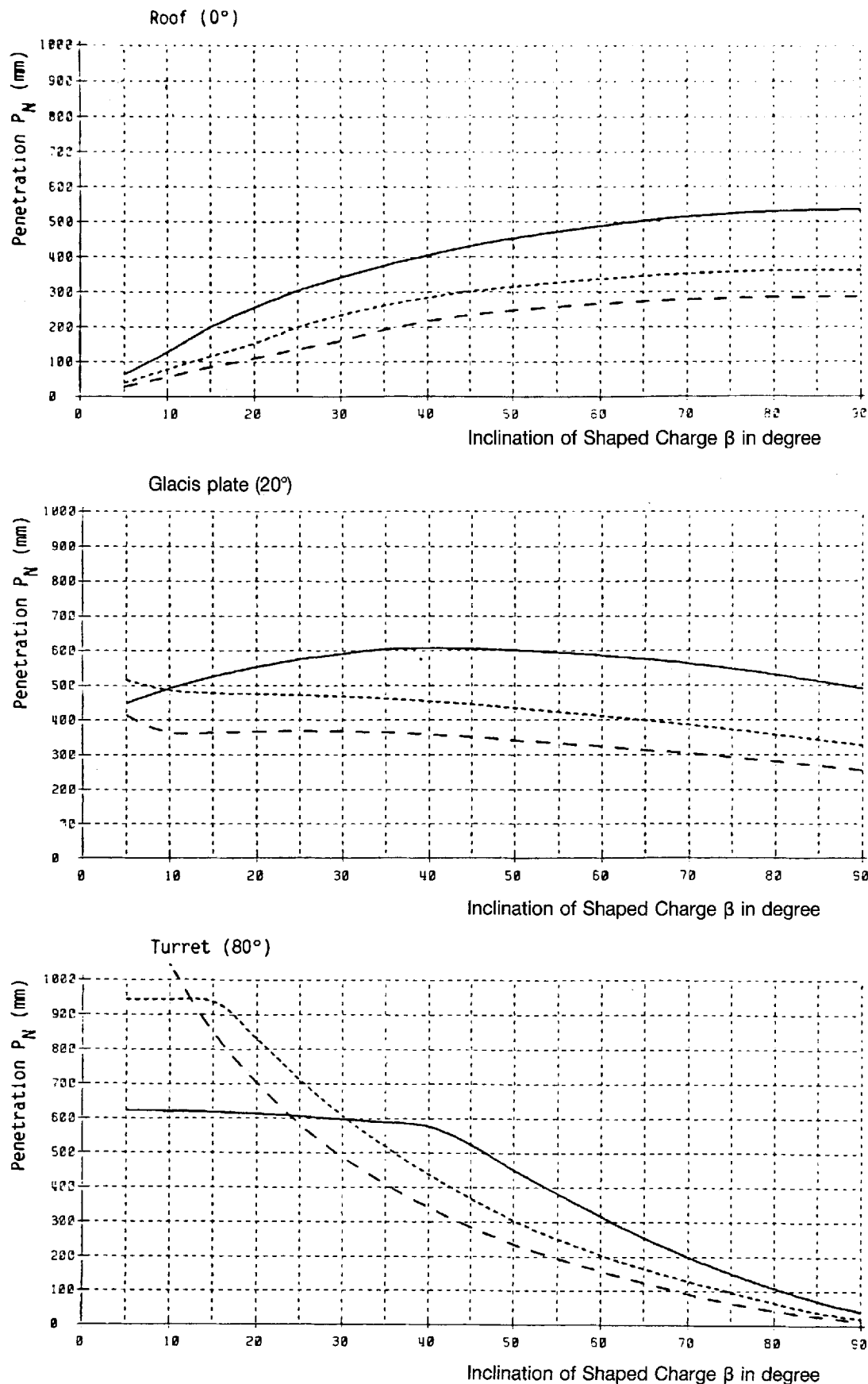


**Figure 6.** Dynamic depths of penetration normal to the plate,  $P_N$ , in target plates with  $0^\circ$  (roof),  $20^\circ$  (glacis plate) and  $80^\circ$  (turret) as a function of the angle of inclination,  $\beta$ , of the shaped charge with respect to the flight direction of the carrier system, which moves horizontally at a speed of 300 m/s, for distances of 300 (—), 600 (----) and 900 mm (— · —) from the virtual origin of the shaped charge to the target surface.

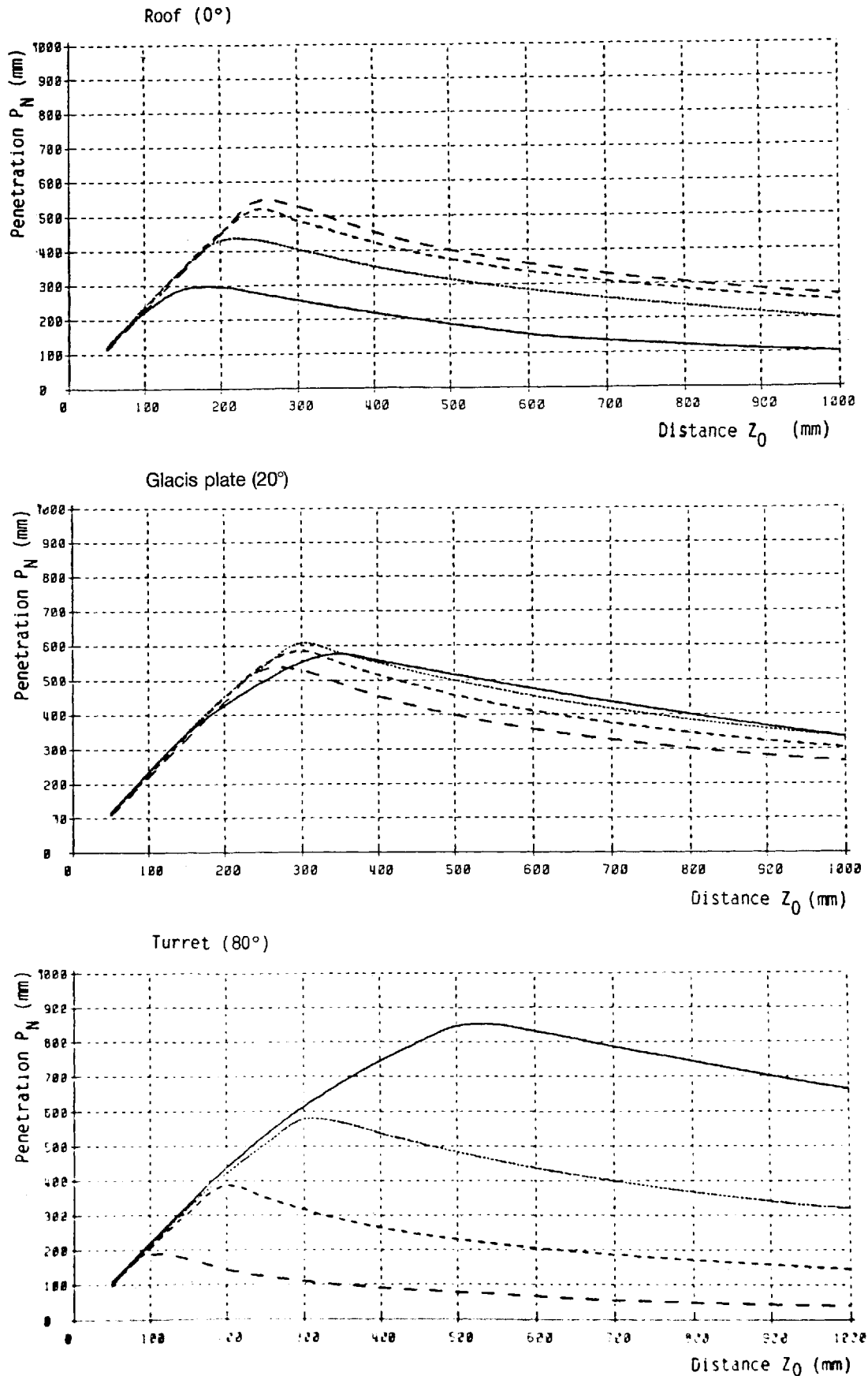


**Figure 7.** Dynamic depths of penetration,  $P_N$ , in target plates with 0° (roof), 20° (glacis plate) and 80° (turret) as a function of the distance from the virtual origin, the inclinations  $\beta$  of the shaped charge being 20° (—), 40° (·····), 60° (----) and 80° (-·-·-) with respect to the direction of flight, and with the missile flying horizontally at a speed of 300 m/s.

|                                  |                            |
|----------------------------------|----------------------------|
| missile velocity $v_m$           | 300 m/s or 0.3 mm/ $\mu$ s |
| missile direction, $\alpha$      | 0°                         |
| jet tip velocity, $v_j^1$        | 9 mm/ $\mu$ s              |
| particulated jet diameter, $D_p$ | 3 mm                       |
| break-up time, $t_p$             | 200 $\mu$ s                |
| KE/V-factor, K                   | 0.07 cm <sup>3</sup> /J    |

The Table below (Fig. 5) is part of the computer printout. The angle of inclination  $\beta$  of the shaped charge is being varied here, whereas the angle of the missile axis  $\alpha$  is kept constant at 0°. Also, a horizontal target plate with angle  $\varepsilon$  equal to 0° is considered. First, the distances  $Z_0$  and  $Z_1$  are calculated. The next columns then give  $v_{j,\beta}^1$ ,  $v_{j,\beta}^\perp$ ,  $v_{j,\beta}^n$ ,  $x_c$ ,  $P_{dyn}$  and  $P_N$ .

The minimum velocity  $v_{j,\beta}^n$  for penetration of the jet in the static case in rolled homogeneous armor is always taken to be 3 mm/ $\mu$ s, if the minimum velocity,  $v_{j,\beta}^n$  due to the cutting effect, is below 3 mm/ $\mu$ s. The examples presented here show, that for the minimum velocity,  $v_{j,\beta}^n$ , the limiting conditions are always given by the crater diameter, because  $v_{j,\beta}^n$  is never 3 mm/ $\mu$ s.

This analytic computer program assumes an ideal jet without any deviation of the individual jet elements from the axis and without any tumbling or lateral drifting of the particles. However, this is sufficient for predicting trends and an optimum configuration of a shaped charge, in particular since certain adaptations to the practical case can be made via the V/KE-factor K.

As shown in Fig. 6, the depth of penetration in the tank roof target,  $\varepsilon = 0^\circ$ , in the direction of the normal to the plate increases with the angle of inclination,  $\beta$ , of the shaped charge and with the vertical distance from the virtual origin,  $Z_0$ , to the target plate ( $Z_0 = 300$  mm, 600 mm and 900 mm) as a parameter.

Surprisingly, the perforation performance against the 20° inclined armor remains more or less constant as the angle of inclination varies from 0° to 90° for the distance between the virtual origin and the target surface is kept constant.

In contrast to this, the depth of penetration in the turret armor, with its 80° obliquity, decreases rapidly with increasing angle  $\beta$ . This is readily understood, because, apart from the incipient cutting effect, the direction of the crater deviates more and more from the normal to the target plate.

In Fig. 7, the dynamic depth of penetration  $P_N$  in the direction of the normal to the target plate is given as a function of the distance  $Z_0$ , with the shaped charge inclination angle  $\beta$  (20°, 40°, 60° and 80°) as a parameter. The other parameters, such as overfly velocity, jet tip velocity  $v_j^1$ , jet diameter  $D_p$  and break-up time  $t_p$ , are the same as in the previous example. Here it is obvious, that the optimum distance for a horizontal target plate, with the missile flying horizontally and the charge dimensions given, is about 250 mm, at least if the charge is inclined at wide angles. This favourable value decreases somewhat at an angle  $\beta = 40^\circ$ , shifting slightly towards shorter distances of 200 mm. This effect becomes more distinct at an angle  $\beta = 20^\circ$ , where the optimum distance is below 200 mm.

It is astonishing, that the depth of penetration in the glacis plate initially increases linearly with distance, the values being more or less the same regardless whether the shaped charge is inclined at 80°, 60°, 40° or 20° to the horizontal.

The 20° inclined charge is certainly the best suited against an inclined target plate of 80°. The optimum stand-off distance being 500 mm for this case. The shaped charge inclined at 60° is much less adequate. This is reasonable, because the obliquity of the plate with respect to the jet axis is rather unfavourable. This effect is considerably more distinct with the shaped

charge inclined at 80°, where the jet virtually scratches the plate surface and the cutting action begins very soon.

## 6. Conclusion

An analytical model has been established for the calculation of the dynamic penetration of inclined shaped charges at an arbitrary stand-off distance and for all possible angles between the shaped charge axis and the axis of the carrier, and for various obliquities of the target plate. For this analysis, a perfect shaped charge jet has been assumed, without any deviation of the jet from the axis and without any drift and tumbling motion of the individual jet particles after break-up of the jet.

For simplicity, the jet has also been assumed to emerge from a virtual origin, and breaks up at a constant time. A modification, taking into account a jet generation across a collapse distance as well as different break-up times along the jet, can be incorporated without any major difficulty, but gives no significant improvement.

The model can be adapted to the experimental results through a modified V/KE-factor K, which must be determined from the experiment for a typical charge configuration. It has been demonstrated in Ref. 1, that many different test results can be described rather well by means of this formula, when this constant has been determined from experiment.

## 7. References

- (1) M. Held, "Transverse Shaped Charges", *8th International Symposium on Ballistics*, Orlando/Florida, 1984, [Proc.] Section VII, pp. VII 39–47.
- (2) R. C. Golestworthy and I. Townsend, "Analytical Model of Shaped Charge Penetration in the Direct and Overflying Top Attack Modes". *8th International Symposium on Ballistics*, Orlando/Florida, 1984, [Proc.] Section VII, pp. VII 1–14.
- (3) I. A. Smith, "Shaped Charge Penetration at Long Standoff", DEAG-1060, Eglin Air Force Base, Florida, 1980, [Proc.] pp. 280–304.

## Nomenclature

|                 |  |
|-----------------|--|
| D               | = Diameter   |
| $D_C$           | = Charge diameter  |
| $D_p$           | = Particle or jet-diameter   |
| $D_T$           | = Diameter of the crater in the target   |
| K               | = Proportionality factor between crater volume and kinetic energy of jet or, short, V/KE-factor.                                 |
| P               | = Penetration  |
| $P_{dyn}$       | = Dynamic penetration depth  |
| $P_N$           | = Dynamic penetration depth normal to the plate surface  |
| t               | = Flight time of the jet particle  |
| $t_1$           | = Flight time of the tip of the jet between virtual origin and target surface  |
| $t_i$           | = Flight time of the i-th jet particle   |
| $t_p$           | = Time of particulation of the jet   |
| $t_{p,s}$       | = Scaled particulation time of the jet ( $t_p/D_C$ )   |
| $v_j$           | = Jet velocity   |
| $v_{j,\perp}$   | = Component of vector sum of jet and missile velocities perpendicular to shaped charge axis                                      |
| $v_{j,\beta}^1$ | = Sum of jet tip velocity and component of missile velocity in direction of shaped charge axis                                   |
| $v_{j,\beta}^n$ | = Sum of jet (particle)-velocity and component of missile velocity in direction of shaped charge axis ( $v_m \cdot \cos \beta$ ) |
| $v_m$           | = Missile (projectile) velocity  |
| $v_{m,\perp}$   | = $v_m \cdot \sin \beta$   |

- $x_c$  = Length of cut on the target plate perpendicular to the original jet axis  
 $x_1$  = Deviation of the tip of the jet on the target plate perpendicular to the shaped charge axis  
 $x_i$  = Deviation of the  $i$ -th jet-particle perpendicular to the shaped charge axis  
 $x_n$  = Deviation of  $n$ -th jet particle on the target plate perpendicular to the shaped charge axis  
 $Z_0$  = Distance between virtual origin of shaped charge and target at time of jet generation in the direction of shaped charge axis  
 $Z_i$  = Component of the trajectory of the  $i$ -th particle parallel to  $Z_0$   
 $Z_1$  = See Fig. 3  
 $Z_n$  = See Fig. 3
- $\alpha$  = Inclination of the missile axis to the horizontal  
 $\beta$  = Inclination of the shaped charge axis with respect to the missile axis  
 $\gamma = \sqrt{\rho_T/\rho_j} = \sqrt{\text{density of target/density of jet}}$   
 $\varepsilon$  = Inclination angle of target plate to the horizontal  
 $\delta = \alpha + \beta + \varepsilon$  (positive angles in clockwise direction)  
 $\rho_j$  = density of jet material  
 $\rho_T$  = density of target material

(Received February 7, 1986; Ms 4/86)